

1 Leaf traits drive differences in biomass partitioning among
2 major plant functional types

3 Remko A. Duursma¹ and Daniel S. Falster²

4 ¹Hawkesbury Institute for the Environment, University of Western Sydney, Locked
5 Bag 1797, Penrith, NSW 2751, Australia

6 ²Biological Sciences, Macquarie University, North Ryde, NSW 2109, Australia

7 August 25, 2015

8 **Summary**

- 9 1. The partitioning of biomass into leaves and stems is one of the most uncertain and influential com-
10 ponents of global vegetation models (GVMs). Although GVMs typically assume that the major
11 woody plant functional types (PFTs) differ in biomass partitioning, empirical studies have not been
12 able to justify these differences. Here we test for differences between PFTs in partitioning of biomass
13 between leaves and stems.
- 14 2. We use the recently published Biomass And Allometry Database (BAAD), a large database includ-
15 ing observations for individual plants. The database covers the global climate space, allowing us to
16 test for direct climate effects in addition to PFT.
- 17 3. The leaf mass fraction (LMF, leaf / total aboveground biomass) varied strongly between PFTs (as
18 defined by deciduous vs. evergreen and gymnosperm vs. angiosperm). We found that LMF, once
19 corrected for plant height, was proportional to leaf mass per area across PFTs. As a result, the PFTs
20 did not differ in the amount of leaf area supported per unit above ground biomass. We found only
21 weak and inconsistent effects of climate on biomass partitioning.
- 22 4. Combined, these results uncover fundamental rules in how plants are constructed and allow for
23 systematic benchmarking of biomass partitioning routines in GVMs.

24 *Keywords:* allocation, plant allometry, biomass estimation, specific leaf area, dynamic global vegetation
25 model

26 Introduction

27 The partitioning of forest biomass among leaves and stems strongly influences the productivity and car-
28 bon cycle of the world's vegetation (Ise *et al.*, 2010; De Kauwe *et al.*, 2014; Friend *et al.*, 2014). Biomass
29 stored in woody stems has a long residence time (Luysaert *et al.*, 2008), whereas leaf biomass turns over
30 quickly, entering the soil carbon cycle where the majority of carbon is released back to the atmosphere
31 (Ryan & Law, 2005). Globally, forests store approximately 360Pg of carbon in living biomass (Pan *et al.*,
32 2011), equivalent to almost 40 years of current anthropogenic CO₂ emissions (Friedlingstein *et al.*, 2014).
33 Reducing uncertainties about biomass partitioning and carbon residence times in GVMs is therefore a
34 priority for understanding the effects of climate and other environmental change on the global carbon
35 cycle (Friend *et al.*, 2014; De Kauwe *et al.*, 2014; Negrón-Jurez *et al.*, 2015).

36 Perhaps the biggest challenge for GVMs is to capture the combined responses of the more than 250,000
37 plant species comprising the world's vegetation. While most plants have the same basic resource require-
38 ments and physiological function, large differences exist among species in the amount of energy invested
39 in different tissues (leaves, stems, roots). The approach taken by most GVMs for dealing with this func-
40 tional diversity is to consider only a few archetypal plant functional types (PFTs) (Harrison *et al.*, 2010;
41 Wullschleger *et al.*, 2014), assumed to differ in key physiological attributes. While GVMs assume or pre-
42 dict differences in biomass partitioning between PFTs (Notes S1), these differences are poorly constrained,
43 due to limited available data. Moreover, there is little consensus on how biomass partitioning and allo-
44 cation (see Methods for terminology) should be modelled in GVMs (Franklin *et al.*, 2012; De Kauwe *et al.*,
45 2014; Friend *et al.*, 2014). These shortcomings largely reflect the lack of suitable datasets of global scope
46 with which models can be tested, constrained and compared (Wolf *et al.*, 2011).

47 In this paper we are primarily interested in the distribution of biomass ('partitioning') between leaves
48 and woody stems, an important component of the residence time of carbon in ecosystems (Friend *et al.*,
49 2014). Previous work based on either whole stands (O'Neill & DeAngelis, 1981; Enquist & Niklas, 2002;
50 Reich *et al.*, 2014) and or a mix on stand- and individual-based measurements (Poorter *et al.*, 2012, 2015),
51 reported differences between angiosperms and gymnosperms in the amount of leaf biomass per unit
52 above-ground biomass (the 'leaf mass fraction', LMF). Poorter *et al.* (2012) and Enquist & Niklas (2002)
53 attributed higher LMF in gymnosperms to longer leaf lifespan (LL) compared to typical angiosperms, but
54 this begs the question whether differences in LMF are also apparent between deciduous and evergreen
55 functional types within angiosperms. It is also unknown whether PFTs with higher leaf biomass also
56 have higher total leaf area, which is relevant because leaf area drives total light interception and thus
57 productivity. Some oft-cited studies have also assumed that gymnosperms carry more leaf area than
58 angiosperms (Chabot & Hicks, 1982; Bond, 1989).

59 Little is known about global-scale patterns in LMF and LAR in relation to climate. It can be expected that
60 biomass partitioning is correlated with precipitation or mean annual temperature because smaller-scale

61 comparisons have shown responsiveness of biomass partitioning to environmental drivers (Berninger &
62 Nikinmaa, 1994; Callaway *et al.*, 1994; Delucia *et al.*, 2000; Poyatos *et al.*, 2007). Moreover, a recent study by
63 Reich *et al.* (2014) demonstrated that stand-scale biomass partitioning was related to mean annual temper-
64 ature across diverse forest stands. Indeed, many GVMs assume that climate affects biomass partitioning
65 within a given PFT, often through soil water stress or other abiotic stress factors (see Notes S1). Again,
66 however, these models do not agree on the degree of plasticity in biomass partitioning, or which climate
67 variables it should respond to.

68 Despite considerable advances in theory underlying allometric scaling in plants (Enquist, 2003; West *et al.*,
69 1999; Savage *et al.*, 2010) we do not yet have a clear understanding of potential differences between PFTs in
70 terms of biomass partitioning. Instead, most previous work has focussed on understanding size-related
71 shifts in biomass partitioning, as governed by constraints including hydraulic supply and mechanical
72 stability (Savage *et al.*, 2010). Rather than to advance a specific model of biomass partitioning or alloca-
73 tion, our view is that a broader evidence base is needed first to elucidate patterns between PFTs. This
74 should enable those building GVMs to refine algorithms and parameter values to more closely match
75 the observations. Here, we use a unique, new database (Falster *et al.*, 2015) (Fig. 1) to establish general
76 rules on how biomass partitioning differs among three dominant woody PFTs across the globe: ever-
77 green gymnosperms, evergreen angiosperms, and deciduous angiosperms. A recent compilation of plant
78 biomass data (Poorter *et al.*, 2015) speculated that differences between gymnosperms and angiosperms
79 in distribution of biomass between leaves and stems is related to differences in leaf mass per area. Here
80 we can directly test this hypothesis as our database, unlike those of Enquist & Niklas (2002), Reich *et al.*
81 (2014), and Poorter *et al.* (2015), includes many observations of leaf area as well as leaf mass measured on
82 the same plants.

83 A second objective was to study relationships between biomass partitioning and climate variables or
84 biome at a global scale. The dataset includes observations of biomass and size metrics for individual
85 plants, compiled from 175 studies across nine vegetation types (Fig. S1), across the three major biomes
86 (boreal, temperate and tropical). In this paper we focus on field-grown woody plants, spanning the entire
87 size range of woody plants (0.01 - >100 m height). One key challenge is thus to account for the very
88 large size variation commonly found in any allometric variable (Niklas, 1994). We do this by fitting a
89 semi-parametric data-driven statistical model, i.e. one that does not assume a particular functional form,
90 thereby allowing us to study PFT patterns at a common plant height.

91 **Materials and Methods**

92 **Terminology**

93 The terms 'partitioning' and 'allocation' have been used in various ways, confusing comparisons between
94 studies (Litton *et al.*, 2007). Here, we define biomass partitioning as the actual distribution of biomass be-
95 tween compartments (e.g., leaves vs. stems), and biomass allocation as the proportion of net primary
96 production (NPP) that is allocated to some compartment. The two processes are different because of con-
97 tinuous turnover of biomass, which differs strongly between compartments. We may write (McMurtrie
98 & Wolf, 1983),

$$\frac{dM_i}{dt} = a_i \text{NPP} - \tau_i M_i$$

99 where M_i is the biomass in some compartment (leaves, stems or roots) remaining on the plant, a_i the
100 annual allocation of NPP to that compartment, and τ_i the annual turnover (or loss) of compartment i
101 from the plant. It is thus easy to see that partitioning (M_i/M_T , where M_T is total biomass) can be different
102 from allocation (a_i) because turnover (τ_i) differs between leaf and wood biomass. Here, we present data
103 on biomass partitioning, which can inform models of allocation only when estimates of turnover are
104 available.

105 **Data**

106 We used the recently compiled Biomass And Allometry Database (BAAD) (Falster *et al.*, 2015), which
107 in total includes records for 21084 individuals. The database has very limited overlap ($n = 261$, 1.7 %)
108 with the recent large compilation of Poorter *et al.* (2015) and differs in that measurements are all for
109 individual plants (where Poorter *et al.* (2015) included many stand-based estimates converted back to
110 individuals). In this paper we restrict our analysis to records that include leaf mass (M_F), leaf area (A_F),
111 above-ground woody biomass (M_S), plant height (H), and stem area measured at ground level (A_S), or at
112 breast height (typically 1.3m) (A_{Sbh}) ($n=14860$). The database contains many more variables, for example
113 root biomass for a much smaller subset of studies. Here we limit the analysis to patterns in aboveground
114 biomass distribution. For each analysis, we used different subsets of the data because not all variables
115 were measured in each study. Sample sizes by PFT are summarised in Table 1. We excluded glasshouse
116 and common garden studies, including only field-grown woody plants (including natural vegetation,
117 unmanaged and managed plantations). We considered three PFTs : evergreen angiosperms, evergreen
118 gymnosperms, and deciduous angiosperms. We excluded deciduous gymnosperms because few data
119 were available. All locations were further separated into boreal (including sub-boreal), temperate, and
120 tropical biomes. To assess the coverage of the global climate space by the dataset, we extracted mean

121 annual temperature and precipitation from Worldclim (Hijmans *et al.*, 2005), excluding areas without
122 woody vegetation (taken from the global land cover database GLC-SHARE (Latham *et al.*, 2014)).

123 For the above-ground biomass pools, we calculated the leaf mass fraction (M_F/M_T , where M_T is total
124 above-ground biomass) and leaf area ratio (A_F/M_T). These variables are related by,

$$\text{LMF} = \frac{M_F}{M_T} = \left(\frac{M_F}{A_F} \right) \left(\frac{A_F}{M_T} \right) = \text{LMA} \times \text{LAR}.$$

125 We only used LMA directly estimated for the harvested plants (typically for a subsample of leaves, see
126 Falster *et al.* (2015) for details on the methods for each contributed study). For conifers, leaf area was
127 converted to half-total surface area using the average of a set of published conversion factors (Barclay
128 & Goodman, 2000), with different conversion factors applied to pines (*Pinus* spp.) and non-pines. This
129 conversion was necessary because half-total surface area is most appropriate for comparison to flat leaves
130 (Lang, 1991; Chen & Black, 1992). Stem cross-sectional area was measured either at breast height and/or
131 at the base of the plant. For the subset of the data where both were measured, we estimated basal stem
132 area (A_S) from breast height stem area (A_{Sbh}) using a non-linear regression model, as follows.

133 Using the subset of data where basal stem diameter (A_S) and diameter at breast height (A_{Sbh}) were mea-
134 sured (a total of 1270 observations covering the three major PFTs), we developed a non-linear model to
135 predict A_S when only A_{Sbh} and plant height (H) were measured. We fit the following equation, using
136 non-linear regression.

$$D_S = D_{Sbh} H^a / (H - H_{bh})^a$$

137 where D_S is the basal stem diameter (m), D_{Sbh} stem diameter at breast height, H_{bh} the height at which
138 D_{Sbh} was measured (typically 1.3 or 1.34m), and a was further expressed as a function of plant height:

$$a = c_0 H^{c_1}.$$

139 The estimated coefficients were $c_0 = 0.424$, $c_1 = 0.719$, root-mean square error = 0.0287.

140 Data analysis

141 We used generalised additive models (GAM) to capture the relationships between biomass and plant size
142 variables, and to estimate variables and their confidence intervals such as LMF at a common plant height.
143 In all fitted GAMs, we used a cubic regression spline. For the smoothed term in the model (plant height),
144 we used up to 3 or 4 degrees of freedom, which resulted in biologically realistic smoothed relationships.
145 Within the GAM, we used a penalised regression smoother (Wood, 2006) to allow the final degree of

146 smoothness to be estimated from the data. In all fitted GAMs, we used species-dataset combination as a
147 random effect. All variables (except MAP and MAT) were log-transformed prior to analysis.

148 Variance explained by quantitative climate variables (MAP and MAT) were tested with GAMs where
149 variables were sequentially added to the model, and the explained variance (R^2) calculated. For the test
150 of biome effects on biomass partitioning, we used a linear mixed-effects model (because two factors and
151 their interactions were tested), again with species-dataset as the random effect. We calculated the R^2 for
152 linear mixed-effects models for the fixed effects only (Nakagawa & Schielzeth, 2013).

153 Despite the exceptional size of our dataset, the strong size-dependence of LMF still hinders comparisons
154 across climatic gradients, due to the small sample size available within each species or site when sampling
155 at a common height. To study climate effects on biomass partitioning, we therefore further decomposed
156 LMF as the product,

$$\text{LMF} = \left(\frac{M_F}{A_S} \right) \left(\frac{A_S}{M_T} \right). \quad (1)$$

157 This decomposition showed that the vast majority of size-related variation was captured by A_S/M_T alone,
158 indicating that comparisons among M_F/A_S could be made without needing to compare at a common
159 height. A similar decomposition of LAR as the product of A_F/A_S and A_S/M_T produced the same out-
160 come. We therefore analysed for climatic effects on M_F/A_S and A_F/A_S in two ways: with quantitative
161 variables (mean annual precipitation, MAP; mean annual temperature, MAT), and by biome (tropical /
162 temperate/ boreal), a simple classification taking into account both MAT and MAP (Fig. S1). In both
163 cases we used PFT and plant height as covariates varying across climate space.

164 All analyses were conducted in R v3.2.0 (R Core Team, 2015). GAMs were fitted using *mgcv* package
165 (Wood, 2006). The code to replicate this analysis are available on GitHub at <http://github.com/RemkoDuursma/baadana>

166 Results

167 The raw data in Fig. 2 show a steeper increase of woody aboveground biomass (M_S) with plant height
168 compared to foliage biomass (M_F). As a result, LMF decreased with plant height, with the three plant
169 functional types clearly differing in LMF across nearly the entire size range (Fig. 3a). When we corrected
170 for plant height by estimating LMF at a common plant height, we found that LMF was proportional to the
171 average leaf mass per area (LMA) across the three PFTs (Fig. 3b). As a consequence, LAR was invariant
172 between PFTs, because $\text{LAR} = \text{LMF} / \text{LMA}$ (Fig. 3c and Fig. S2).

173 Mirroring the results for LMF, we found that the amount of leaf mass per unit stem area (M_F/A_S) differed
174 among the three PFTs, that these differences were also proportional to LMA (Fig. 3d), and that PFTs were
175 similarly invariant in the amount of leaf area per unit stem area (A_F/A_S) (Fig. 3e).

176 The above results highlight how LMA drives differences in biomass partitioning among dominant woody
177 PFTs. To assess whether LMA could replace PFT when predicting biomass partitioning, we fit a linear
178 mixed-effects model to LMF and M_F/A_S using PFT and plant height (and the quadratic term) as predic-
179 tors (and all interactions). We then replaced PFT with LMA, and found that the model with LMA could
180 explain almost as much variation in LMF as the model with PFT ($R^2 = 0.74$ with PFT vs. 0.62 with LMA),
181 likewise for M_F/A_S ($R^2 = 0.29$ vs. 0.28).

182 There was considerable variation in all studied variables between species within PFTs (Fig. 4). To
183 understand whether we can improve on a PFT-based classification by including other traits that affect
184 biomass partitioning, we decomposed M_F/A_S into LMA (M_F/A_F), and the ratio of leaf area to stem
185 cross-sectional area (A_F/A_S):

$$\frac{M_F}{A_S} = \left(\frac{M_F}{A_F} \right) \left(\frac{A_F}{A_S} \right). \quad (2)$$

186 The ratio M_F/A_S is relevant because plant leaf mass is frequently estimated from A_S with allometric
187 equations (Shinozaki *et al.*, 1964; Chave *et al.*, 2005), using records of stem diameter commonly recorded
188 on long-term monitoring plots. The correlation between M_F/A_S and LMA was found to hold also within
189 PFTs (Fig. 5a), explaining 30% of the variation in M_F/A_S across species. The regressions across species
190 by PFT were broad and overlapping, with a more general relationship extending across the entire LMA
191 axis. A larger fraction of the variation in M_F/A_S was explained by species-level differences in A_F/A_S
192 (Fig. 5b). As previously noted, A_F/A_S does not differ systematically among PFTs (Fig. 3e), but does vary
193 close to two orders of magnitude across species. In Fig. 5b, the separation among PFTs in M_F/A_S arises
194 due to differences in LMA.

195 We found that decomposing LMF and LAR as shown in Eq. 1 was very useful to study climate effects
196 because the second term (A_S/M_T) absorbed nearly all of the size-related variation in LMF (Table 2 and
197 Fig. S3) and is otherwise fairly conserved across PFTs (Fig. S3). As shown in Fig. 5b and Fig. 3d, the
198 term M_F/A_S exhibits comparable differences between PFTs to LMF, but unlike LMF, M_F/A_S is nearly
199 independent of plant height (Table 2). M_F/A_S is thus a useful proxy for LMF that can be compared
200 across species and sites.

201 Regardless of how we analysed the data, we found only weak climatic effects on biomass partitioning
202 within PFTs (Fig. 6). Biome consistently explained very little variation when added to a statistical model
203 in addition to PFT and plant height (R^2 increased by only 0.01 - 0.06, see Table 2). Likewise, we found
204 weak and inconsistent effects of climate variables (MAP and MAT) (Fig. 6b-c). These variables explained
205 little variation when added to a statistical model in addition to PFT and plant height (R^2 increased by
206 0.01 and 0.11, respectively, see Table 2).

207 Discussion

208 We found that PFTs differed in LMF, and that LMF was proportional to LMA. This conclusion was par-
209 ticularly strong across the three PFTs studied, but it also held across species within PFT. The implication
210 is that the amount of leaf area supported per unit biomass (leaf area ratio, LAR) does not differ between
211 PFTs. This result seems robust, as our data include individual plants spanning the entire size range of
212 woody plants in natural forests (0.1-100m) (Fig. 3a). Previous studies have demonstrated a large differ-
213 ence in LMF between angiosperms and gymnosperms (Poorter *et al.*, 2012, 2015), but have not been able
214 to explain these differences in terms of leaf traits. We show that LMA – a central trait of the leaf economics
215 spectrum (LES) (Wright *et al.*, 2004) – explains differences in LMF in a consistent manner.

216 We found that, as expected, plant size strongly influences LMF (Fig. 3) and LAR (Fig. S2) (see also Poorter
217 *et al.* (2012, 2015)). It is thus necessary to correct for plant size when comparing biomass partitioning pa-
218 rameters, as has been noted many times (McConnaughay & Coleman, 1999). We used a semi-parametric
219 approach to account for plant size, which has the advantage that it does not require an *a priori* assump-
220 tion on the functional relationship. This was useful because both LMF and LAR showed very non-linear
221 patterns with plant height, even on a logarithmic scale, consistent with recent other results (Poorter *et al.*,
222 2015).

223 The finding that LMF is proportional to LMA across PFTs implies that LAR does not differ systematically
224 between PFTs. One explanation for this pattern lies in the strong positive correlation between LMA and
225 leaf lifespan (LL) (Wright *et al.*, 2004). Both Poorter *et al.* (2012) and Enquist & Niklas (2002) explained
226 higher LMF in gymnosperms by higher LL; plants simply maintain more cohorts of foliage, but this
227 explanation demands that all else is equal. Yet it is not self-evident that everything else is indeed equal,
228 that is, annual production of foliage could differ between PFTs. Nonetheless, further supporting this
229 explanation, Reich *et al.* (1992) showed a positive correlation between LL and total stand leaf biomass
230 across diverse forest stands. Another, not mutually exclusive, possible explanation is that plants may
231 allocate biomass in a manner that targets a more constant LAR rather than LMF. Canopy size scales with
232 M_T (Duursma *et al.*, 2010), and a larger canopy means higher light interception per unit total biomass
233 (Duursma & Mäkelä, 2007). It can thus be argued that an optimal LAR exists that balances investment in
234 supporting woody biomass (reflected by M_T) and the efficiency of foliage in terms of light interception.

235 We found that patterns in M_F/A_S across PFTs mirrored those of LMF (Fig. 3). Because LMF may be
236 decomposed into the terms M_F/A_S and M_T/A_S (eq. 2), this result suggests that M_T/A_S does not vary
237 between PFTs (see also Fig. S3). If this result holds, it means that aboveground biomass may be estimated
238 across PFTs with a single equation that does not differ between PFTs. For tropical forests, Chave *et al.*
239 (2005) showed that aboveground biomass can be estimated as,

$$M_T = F\rho A_S H_T$$

240 where F is a form factor, and ρ wood density (kg m^3). After rearranging, this equation predicts that
241 M_T/A_S is proportional to plant height. We found some support for this prediction (Fig. S3), suggesting
242 further improvements could be made by incorporating this dependence. It is timely to use database
243 made public by Falster *et al.* (2015) (BAAD) and Poorter *et al.* (2015) to develop more general equations to
244 estimate individual plant aboveground biomass across the globe.

245 We found that climate did not appreciably affect biomass partitioning between leaves and stems. This
246 finding is in contrast with a recent study where LMF was found to increase with MAT across the globe
247 (Reich *et al.*, 2014). One explanation for this difference is that our measurements were taken on individual
248 plants, whereas in Reich *et al.* (2014) they were on whole stands. This suggests climatic effects on stand-
249 level biomass partitioning occur primarily by altering the size-distribution and stand density (number of
250 individuals per unit area), rather than partitioning within individual plants. With the caveats that there
251 is still variation between species and studies unaccounted for (Fig. 4), and that coarse climate variables
252 such as MAT and MAP may mask small-scale climate effects on biomass partitioning, our results strongly
253 suggest the effects of PFT are stronger than any direct climate effect on biomass partitioning within indi-
254 vidual plants (Table 2).

255 Our results indicate that it is possible to integrate a key leaf trait with whole-plant modelling of biomass
256 partitioning. Indeed, nearly as much variation was explained across species when using LMA instead of
257 PFT in a statistical model. This is surprising because LMA only captures one aspect of functional differen-
258 tiation among PFT – leaf morphology (but including correlated effects on leaf lifespan and photosynthetic
259 capacity via the leaf economics spectrum (Wright *et al.*, 2004)). We thus show that in a PFT-based classi-
260 fication, LMA is a good first estimate of biomass partitioning, however, more variation can be explained
261 by another trait (A_F/A_S), which varies appreciably between species. These results suggest promising
262 avenues for parameterising and simplifying biomass partitioning routines in GVMs.

263 Overall, our results establish general patterns about plant construction and thus lay an empirical base
264 against which models can be benchmarked. A recent study compared allocation routines in a number of
265 leading ecosystem models (De Kauwe *et al.*, 2014), and recommended constraining allocation by observed
266 biomass fractions instead of using constant allocation fractions. Based on our findings, a first approxima-
267 tion within GVMs would be to assume leaf area to stem cross-sectional area a parameter that does not
268 vary between PFTs (notwithstanding effects of plant height on this variable), and vary biomass alloca-
269 tion accordingly. LMA, already a parameter in most GVMs, then gives the ratio of leaf biomass to stem
270 area. Some models already incorporate a similar algorithm (see Notes S1), while other algorithms may be
271 tuned to yield similar patterns between PFTs as we have presented. In any case, the growing availability
272 of large datasets on stand biomass and individual plant construction (Falster *et al.*, 2015) suggest the time
273 is ripe for rigorous benchmarking (Abramowitz, 2012; De Kauwe *et al.*, 2014) of GVMs against empirical
274 data.

275 **Acknowledgments**

276 Our sincere thanks to everyone who contributed data to the Biomass and Allometry Database. We thank
277 Martin De Kauwe and anonymous referees for comments on an earlier version of this paper. Thanks also
278 to Rich FitzJohn for advice about using the remake package. Figure 2a uses an image by Lana Heydon,
279 IAN Image Library <http://ian.umces.edu/imagelibrary>.

280 Tables

Table 1 Sample sizes used in the analyses of the four variables considered in the study by plant functional type (PFT, DA = deciduous angiosperm, EA = evergreen angiosperm, EG = evergreen gymnosperm) and biome. Sample sizes denote number of individuals, with number of unique species in parentheses.

Variable	PFT	boreal	temperate	tropical	Sum
M_F/M_T	DA	184 (4)	1975 (94)	162 (14)	2321 (112)
	EA		1271 (68)	1674 (169)	2945 (237)
	EG	669 (7)	1222 (24)		1891 (31)
	Sum	853 (11)	4468 (186)	1836 (183)	7157 (380)
A_F/M_T	DA		1452 (68)	35 (7)	1487 (75)
	EA		1124 (59)	1320 (112)	2444 (171)
	EG	321 (7)	573 (15)		894 (22)
	Sum	321 (7)	3149 (142)	1355 (119)	4825 (268)
M_F/A_S	DA	308 (6)	2067 (93)	162 (14)	2537 (113)
	EA		1094 (59)	1696 (173)	2790 (232)
	EG	1010 (10)	1896 (31)		2906 (41)
	Sum	1318 (16)	5057 (183)	1858 (187)	8233 (386)
A_F/A_S	DA		1572 (70)	35 (5)	1607 (75)
	EA		970 (54)	1370 (120)	2340 (174)
	EG	458 (8)	1139 (21)		1597 (29)
	Sum	458 (8)	3681 (145)	1405 (125)	5544 (278)

Table 2 Explained variance by plant functional type (PFT), plant height (H) and climate variables (either biome (B), or MAP and MAT) for five whole-plant variables. For the analysis with biome, each variable was added to a linear mixed-effects model, using species within dataset as a random effect. The R^2 shown is that explained by the fixed effects only. All fixed effects were highly significant ($P < 0.001$). In addition to the fixed effects shown, all interactions were added to each of the models. For the analysis with continuous climate variables MAP and MAT, each variable was added as a smooth term in a generalized additive model (GAM), with the exception of PFT (a categorical variable). Note that explained variance for the linear mixed-effects model and GAM is not necessarily the same even with the same predictors, due to different methods for fitting and estimating the explained variance.

Mixed-effects model		Predictors		
Variable	H	H, PFT	H, PFT, B	
Leaf mass fraction(M_F/M_T)	0.65	0.75	0.76	
Leaf area ratio(A_F/M_T)	0.69	0.69	0.75	
Leaf mass / stem basal area(M_F/A_S)	0.01	0.25	0.29	
Leaf area / stem basal area(A_F/A_S)	0.01	0.03	0.05	
Leaf mass per area(M_F/A_F)	0.13	0.60	0.66	
GAM		Predictors		
Variable	H	H, PFT	H, PFT, MAT, MAP	
Leaf mass fraction(M_F/M_T)	0.65	0.76	0.74	
Leaf area ratio(A_F/M_T)	0.69	0.71	0.73	
Leaf mass / stem basal area(M_F/A_S)	0.03	0.24	0.25	
Leaf area / stem basal area(A_F/A_S)	0.05	0.12	0.23	
Leaf mass per area(M_F/A_F)	0.12	0.47	0.61	

281 1 Figures

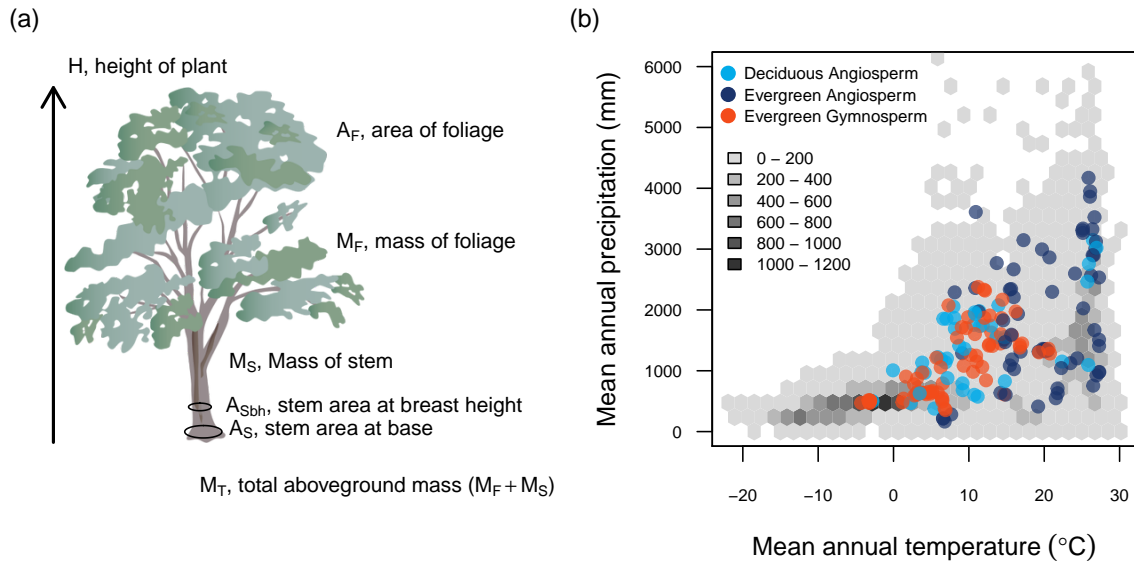


Fig. 1 Overview of the data. (a) Variables were measured on up to 14860 individual plants from 603 species. (b) Coverage of the dataset across global climate space. Grey hexagons indicate the number of 0.5° cells with woody vegetation across the space. Colour symbols show the locations of sampled individuals for three dominant woody functional types.

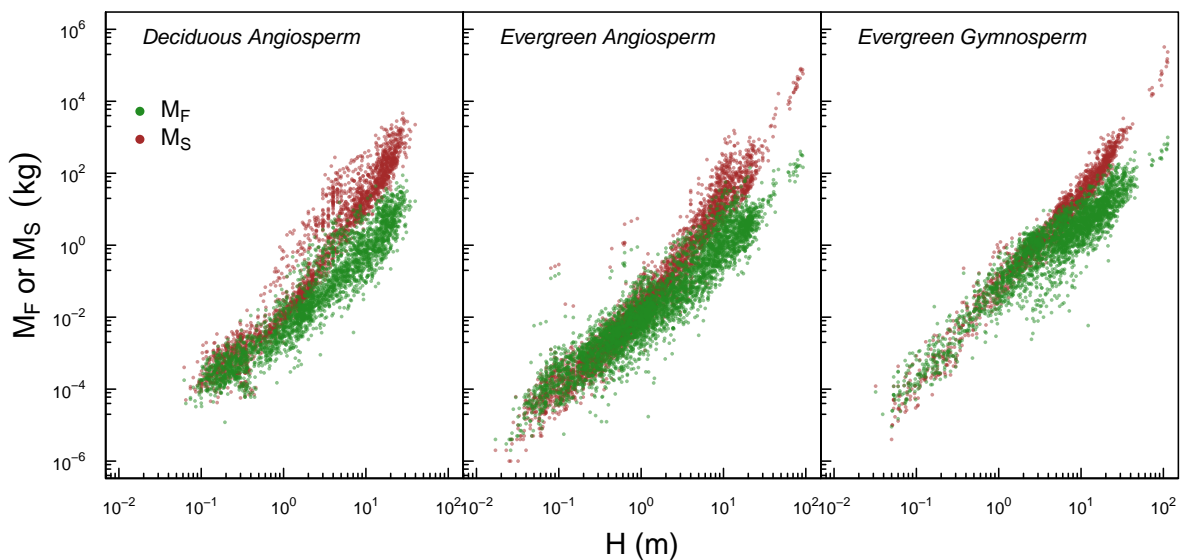


Fig. 2 Raw data for leaf biomass (M_F) and total above-ground woody biomass (M_S) for each of the PFTs, as a function of total plant height (H). Each point is an individual plant. Sample sizes are listed in Table 1

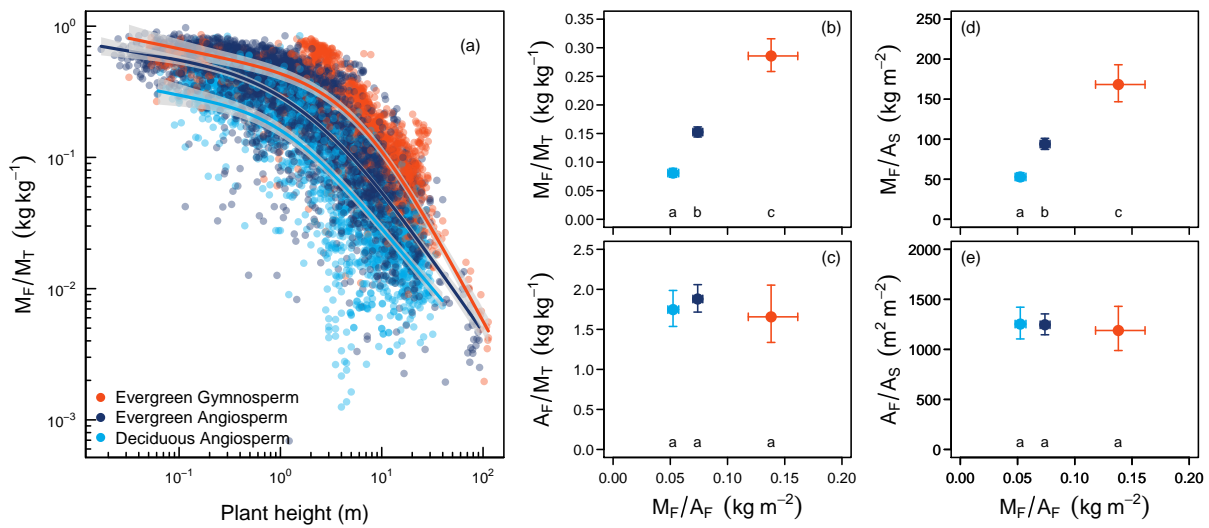


Fig. 3 Dominant woody PFTs differ in leaf mass fraction due to underlying differences in leaf mass per area. (a) Leaf mass fraction (M_F/M_T = leaf mass / above-ground biomass) by PFT. Each symbol is an individual plant. Lines are generalised additive model fits. (b) and (c) Leaf mass fraction and leaf area ratio (A_F/M_T) at the average plant height in the dataset, estimated from panel (a). (d) Average leaf mass per unit basal stem area, and (e) leaf area per unit basal stem area for the three major PFTs confirm that the between-PFT variation in leaf mass fraction is due to leaf mass per unit basal area. Error bars are 95% confidence intervals. Letters denote significant differences (at $\alpha = 0.05$).

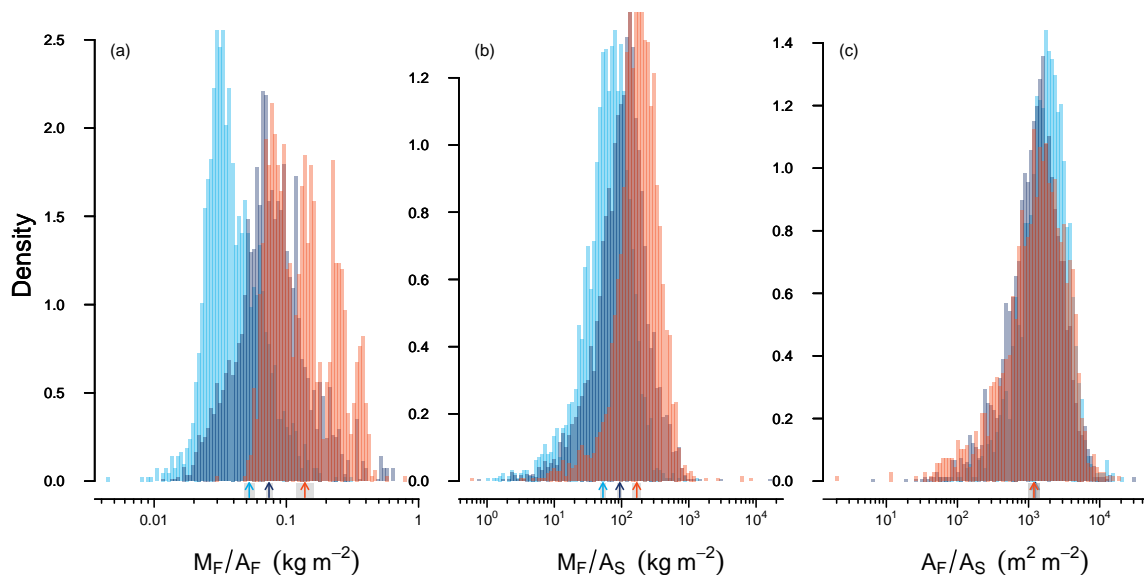


Fig. 4 Plant functional types diverge strongly in mass-based partitioning, but converge in area-based partitioning. Shown are histograms (as probability density functions) of leaf mass per area (M_F/A_F), leaf mass per unit basal stem area (M_F/A_S) and leaf area per unit basal stem area (A_F/A_S) grouped by the three PFTs. Arrows indicate means by PFT. Colours as in Fig. 3.

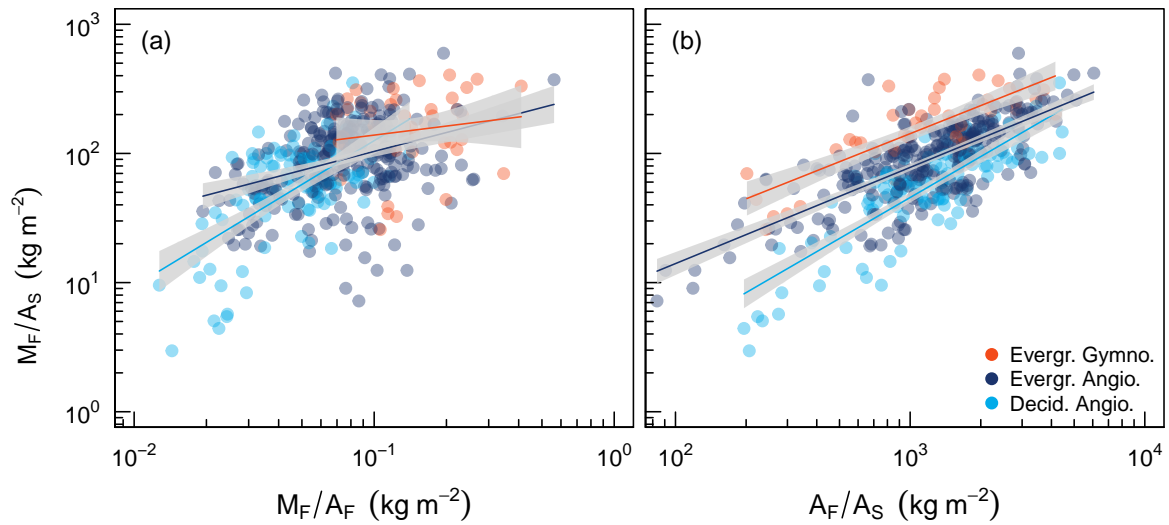


Fig. 5 Leaf and stem traits capture variation in biomass partitioning across species. Individual plant data were averaged by species and study combinations. Lines are linear regressions with 95% confidence intervals. Both regressions were significant ($P < 0.01$). R^2 for fitted relationships are 30.9% in panel (a) and 66% in panel (b) (for a linear regression model including PFT as a factor variable).

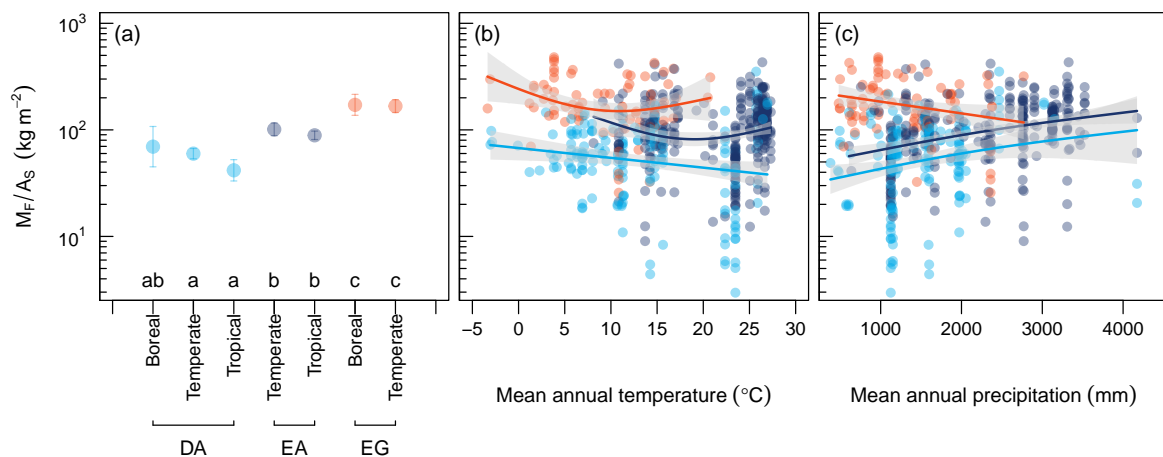


Fig. 6 Beyond influencing the distribution of PFTs, climate only modestly influences biomass partitioning. a) Leaf mass per unit stem cross-sectional area (M_F/A_S) for each PFT within three different biomes. DA: deciduous angiosperms, EA: evergreen angiosperms, EG: evergreen gymnosperms. Error bars are 95% confidence intervals for the mean, estimated from a linear mixed-effects model using species within study as the random effect. Letters denote significant differences (at $\alpha = 0.05$). b-c) Relationships between climate and M_F/A_S within each PFT. Solid lines are generalised additive model (GAM) fits (with a base dimension of 3); with grey areas indicating the 95% confidence interval around the GAM.

References

- 282 **References**
- 283 **Abramowitz G. 2012.** Towards a public, standardized, diagnostic benchmarking system for land surface
284 models. *Geoscientific Model Development*, **5**, 819–827.
- 285 **Barclay H , Goodman D. 2000.** Conversion of total to projected leaf area index in conifers. *Canadian*
286 *Journal of Botany*, **78**, 447–454.
- 287 **Berninger F , Nikinmaa E. 1994.** Foliage area - sapwood area relationships of Scots pine (*Pinus sylvestris*)
288 trees in different climates. *Canadian Journal of Forest Research*, **24**, 2263–2268.
- 289 **Bond WJ. 1989.** The tortoise and the hare: ecology of angiosperm dominance and gymnosperm persis-
290 tence. *Biological Journal of the Linnean Society*, **36**, 227–249.
- 291 **Callaway RM, DeLucia EH , Schlesinger WH. 1994.** Biomass allocation of montane and desert Ponderosa
292 pine: an analog for response to climate change. *Ecology*, **75**, 1474–1481.
- 293 **Chabot BF , Hicks DJ. 1982.** The ecology of leaf life spans. *Annual Review of Ecology and Systematics*, **13**,
294 229–259.
- 295 **Chave J, Andalo C, Brown S, Cairns MA, Chambers JQ, Eamus D, Foelster H, Fromard F, Higuchi N,
296 Kira T *et al.*. 2005.** Tree allometry and improved estimation of carbon stocks and balance in tropical
297 forests. *Oecologia*, **145**, 87–99.
- 298 **Chen JM , Black TA. 1992.** Defining leaf-area index for non-flat leaves. *Plant Cell and Environment*, **15**,
299 421–429.
- 300 **De Kauwe MG, Medlyn BE, Zaehle S, Walker AP, Dietze MC, Wang YP, Luo Y, Jain AK, El-Masri
301 B, Hickler T *et al.*. 2014.** Where does the carbon go? A model-data intercomparison of vegetation
302 carbon allocation and turnover processes at two temperate forest free-air CO₂ enrichment sites. *New*
303 *Phytologist*.
- 304 **Delucia EH, Maherali H , Carey EV. 2000.** Climate-driven changes in biomass allocation in pines. *Global*
305 *Change Biology*, **6**, 587–593.
- 306 **Duursma RA , Mäkelä A. 2007.** Summary models for light interception and light-use efficiency of non-
307 homogeneous canopies. *Tree Physiology*, **27**, 859–870. 6.
- 308 **Duursma RA, Mäkelä A, Reid DEB, Jokela EJ, Porte AJ , Roberts SD. 2010.** Self-shading affects allomet-
309 ric scaling in trees. *Functional Ecology*, **24**, 723–730. 4.
- 310 **Enquist BJ. 2003.** Cope’s rule and the evolution of long-distance transport in vascular plants: allometric
311 scaling, biomass partitioning and optimization. *Plant, Cell & Environment*, **26**, 151–161.
- 312 **Enquist BJ , Niklas KJ. 2002.** Global allocation rules for patterns of biomass partitioning in seed plants.
313 *Science*, **295**, 1517–1520.

- 314 **Falster DS, Duursma RA, Ishihara MI, Barneche DR, FitzJohn RG, Vårhammar A, Aiba M, Ando M,**
315 **Anten N, Aspinwall MJ *et al.*. 2015.** BAAD: a Biomass And Allometry Database for woody plants.
316 *Ecology*, **96**, 1445–1445.
- 317 **Franklin O, Johansson J, Dewar RC, Dieckmann U, McMurtrie RE, Brännström A, Dybzinski R. 2012.**
318 Modeling carbon allocation in trees: a search for principles. *Tree Physiology*, **32**, 648–666.
- 319 **Friedlingstein P, Andrew RM, Rogelj J, Peters GP, Canadell JG, Knutti R, Luderer G, Raupach MR,**
320 **Schaeffer M, van Vuuren DP *et al.*. 2014.** Persistent growth of CO₂ emissions and implications for
321 reaching climate targets. *Nature Geoscience*, **7**, 709–715.
- 322 **Friend AD, Lucht W, Rademacher TT, Keribin R, Betts R, Cadule P, Ciais P, Clark DB, Dankers R, Fal-**
323 **loon PD *et al.*. 2014.** Carbon residence time dominates uncertainty in terrestrial vegetation responses
324 to future climate and atmospheric CO₂. *Proceedings of the National Academy of Sciences*, **111**, 3280–3285.
- 325 **Harrison SP, Prentice IC, Barboni D, Kohfeld KE, Ni J, Sutra JP. 2010.** Ecophysiological and bioclimatic
326 foundations for a global plant functional classification. *Journal of Vegetation Science*, **21**, 300–317.
- 327 **Hijmans RJ, Cameron SE, Parra JL, Jones PG, Jarvis A. 2005.** Very high resolution interpolated climate
328 surfaces for global land areas. *International journal of climatology*, **25**, 1965–1978.
- 329 **Ise T, Litton CM, Giardina CP, Ito A. 2010.** Comparison of modeling approaches for carbon partitioning:
330 impact on estimates of global net primary production and equilibrium biomass of woody vegetation
331 from MODIS GPP. *Journal of Geophysical Research: Biogeosciences*, **115**.
- 332 **Lang ARG. 1991.** Application of some of cauchy's theorems to estimation of surface-areas of leaves,
333 needles and branches of plants, and light transmittance. *Agricultural and Forest Meteorology*, **55**, 191–
334 212.
- 335 **Latham J, Cumani R, Rosati I, Bloise M. 2014.** Global land cover share (glc-share) database beta-release
336 version 1.0-2014. URL: http://www.glcen.org/databases/lc_glcshare_downloads_en.jsp.
- 337 **Litton CM, Raich JW, Ryan MG. 2007.** Carbon allocation in forest ecosystems. *Global Change Biology*, **13**,
338 2089–2109.
- 339 **Luyssaert S, Schulze ED, Boerner A, Knohl A, Hessenmoeller D, Law BE, Ciais P, Grace J. 2008.** Old-
340 growth forests as global carbon sinks. *Nature*, **455**, 213–215.
- 341 **McConnaughay KDM, Coleman JS. 1999.** Biomass allocation in plants: ontogeny or optimality? A test
342 along three resource gradients. *Ecology*, **80**, 2581–2593.
- 343 **McMurtrie R, Wolf L. 1983.** Above- and below-ground growth of forest stands: a carbon budget model.
344 *Annals of Botany*, **52**, 437–448.
- 345 **Nakagawa S, Schielzeth H. 2013.** A general and simple method for obtaining R² from generalized linear
346 mixed-effects models. *Methods in Ecology and Evolution*, **4**, 133–142.

- 347 **Negrón-Jurez RI, Koven CD, Riley WJ, Knox RG , Chambers JQ. 2015.** Observed allocations of pro-
348 ductivity and biomass, and turnover times in tropical forests are not accurately represented in CMIP5
349 earth system models. *Environmental Research Letters*, **10**, 064017.
- 350 **Niklas KJ. 1994.** *Plant allometry: the scaling of form and process*. The University of Chicago Press, Chicago.
- 351 **O'Neill RV , DeAngelis DL. 1981.** Comparative productivity and biomass relations of forest ecosystems.
352 *Dynamic properties of forest ecosystems*, pp. 411–449.
- 353 **Pan Y, Birdsey RA, Fang J, Houghton R, Kauppi PE, Kurz WA, Phillips OL, Shvidenko A, Lewis SL,**
354 **Canadell JG et al.. 2011.** A large and persistent carbon sink in the world's forests. *Science*, **333**, 988–993.
- 355 **Poorter H, Jagodzinski AM, Ruiz-Peinado R, Kuyah S, Luo Y, Oleksyn J, Usoltsev VA, Buckley TN,**
356 **Reich PB , Sack L. 2015.** How does biomass distribution change with size and differ among species?
357 An analysis for 1200 plant species from five continents. *New Phytologist*, p. 10.1111/nph.13571.
- 358 **Poorter H, Niklas KJ, Reich PB, Oleksyn J, Poot P , Mommer L. 2012.** Biomass allocation to leaves,
359 stems and roots: meta-analyses of interspecific variation and environmental control. *New Phytologist*,
360 **193**, 30–50.
- 361 **Poyatos R, Martinez-Vilalta J, Čermák J, Ceulemans R, Granier A, Irvine J, Köstner B, Lagergren F,**
362 **Meiresonne L, Nadezhdina N et al.. 2007.** Plasticity in hydraulic architecture of Scots pine across
363 Eurasia. *Oecologia*, **153**, 245–259.
- 364 **R Core Team. 2015.** *R: a language and environment for statistical computing*. R Foundation for Statistical
365 Computing, Vienna, Austria.
- 366 **Reich PB, Luo Y, Bradford JB, Poorter H, Perry CH , Oleksyn J. 2014.** Temperature drives global patterns
367 in forest biomass distribution in leaves, stems, and roots. *Proceedings of the National Academy of Sciences*,
368 **111**, 13721–13726.
- 369 **Reich PB, Walters MB , Ellsworth DS. 1992.** Leaf life-span in relation to leaf, plant, and stand character-
370 istics among diverse ecosystems. *Ecological Monographs*, **62**, 365–392. 3.
- 371 **Ryan MG , Law BE. 2005.** Interpreting, measuring, and modeling soil respiration. *Biogeochemistry*, **73**,
372 3–27.
- 373 **Savage VM, Bentley LP, Enquist BJ, Sperry JS, Smith DD, Reich PB , von Allmen EI. 2010.** Hydraulic
374 trade-offs and space filling enable better predictions of vascular structure and function in plants. *Pro-*
375 *ceedings of the National Academy of Sciences*, **107**, 22722–22727.
- 376 **Shinozaki K, Hozumi K, K., Yoda , Kira T. 1964.** A quantitative analysis of plant form-the pipe model
377 theory: I. Basic analyses. *Japanese Journal of Ecology*, **14**, 97–105.
- 378 **West GB, Brown JH , Enquist BJ. 1999.** A general model for the structure and allometry of plant vascular
379 systems. *Nature*, **400**, 664–667. 6745.

380 **Wolf A, Ciais P, Bellassen V, Delbart N, Field CB , Berry JA. 2011.** Forest biomass allometry in global
381 land surface models. *Global Biogeochemical Cycles*, **25**.

382 **Wood SN. 2006.** *Generalized additive models: an introduction with R*. Texts in Statistical Science. Chapman
383 & Hall CRC.

384 **Wright IJ, Reich PB, Westoby M, Ackerly DD, Baruch Z, Bongers F, Cavender-Bares J, Chapin T, Cor-**
385 **nelissen JHC, Diemer M *et al.*. 2004.** The worldwide leaf economics spectrum. *Nature*, **428**, 821–827.

386 **Wullschleger SD, Epstein HE, Box EO, Euskirchen ES, Goswami S, Iversen CM, Kattge J, Norby RJ,**
387 **Bodegom PMv , Xu X. 2014.** Plant functional types in Earth system models: past experiences and future
388 directions for application of dynamic vegetation models in high-latitude ecosystems. *Annals of Botany*.

389 **Supporting Information**

390 Additional supporting information may be found in the online version of this article.

391

392 **Fig. S1** Global coverage of the climate space by the dataset, labelled by vegetation type.

393 **Fig. S2** Leaf area ratio (A_F/M_T) by PFT.

394 **Fig. S3** Relationship between above-ground biomass and basal stem area.

395 **Notes S1** Modelling of biomass partitioning in global vegetation models (GVMs)